Martensite in nanocrystalline NiTi shape memory alloys: experiment and modelling

M. Petersmann[1,2], T. Antretter[1], F.D. Fischer[1], C. Gammer[3], M. Kerber[4], T. Waitz[4]

[1]Institute of Mechanics, Montanuniversität, Leoben, Austria
[2]Materials Center Leoben Forschung GmbH, Leoben, Austria
[3]Erich Schmid Institute Leoben, Austrian Academy of Sciences, Leoben, Austria
[4]Physics of Nanostructured Materials, Faculty of Physics, University of Vienna, Vienna, Austria

Motivation for nanocrystalline NiTi

- **Shape memory alloy**
- **Stabilization of austenite (i.e. lower $M_{s,f}$, $A_{s,f}$)**
- **Large reversible elastic strain energy**
- **Novel martensitic morphology / metastable & adaptive martensite**
- **Enhanced properties, e.g. cyclic stability**

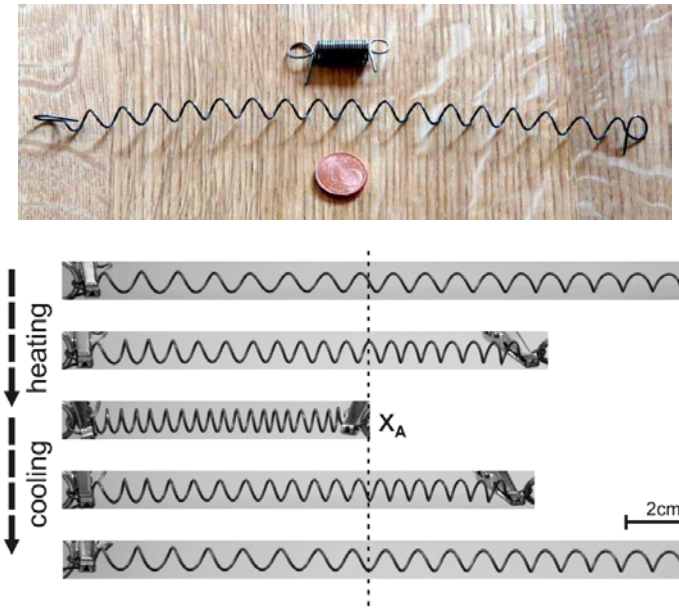

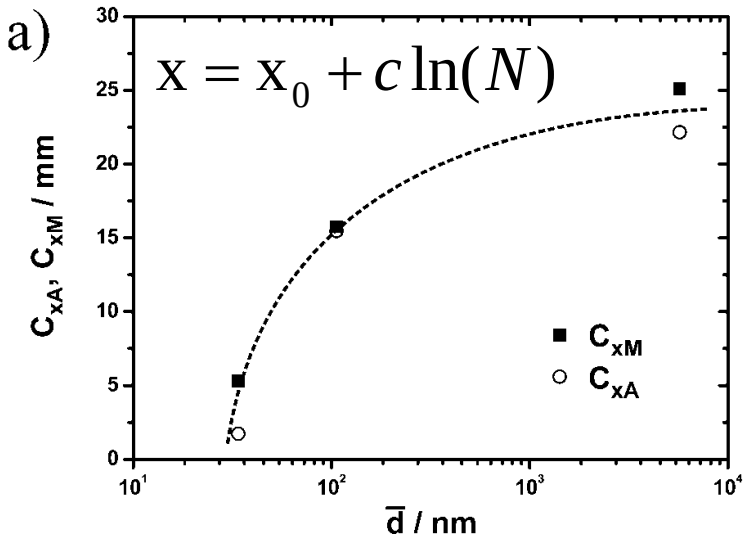

Frenzel et al. (2011)

Geometrically nonlinear theory of martensite formation

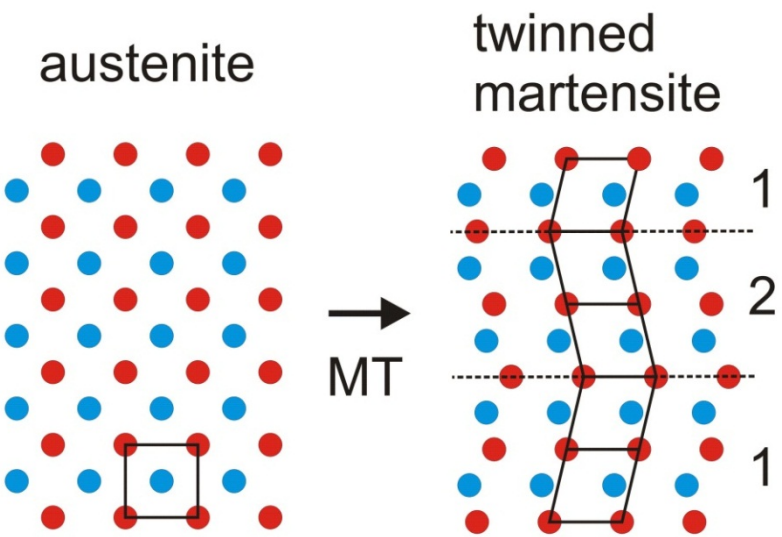

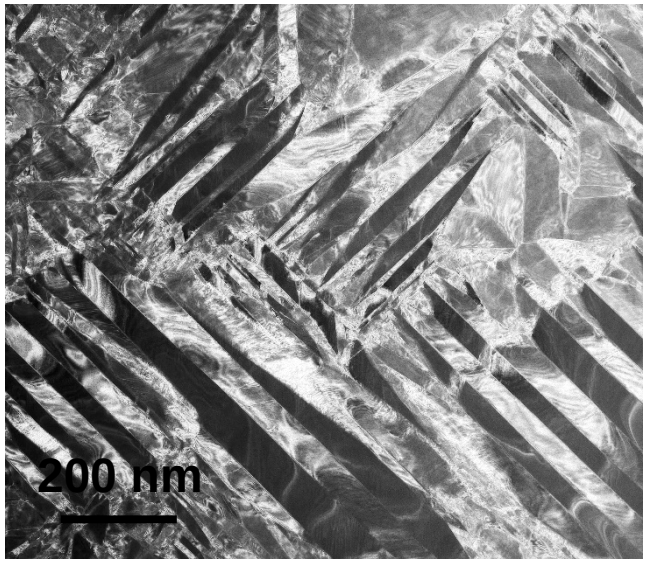

- Minimizing strain by fine mixtures of variants

$$E_{elast} = \int_{\Omega} \varphi(\mathbf{A},\mathbf{B},\ldots)dV$$

$$\mathbf{A},\mathbf{B},\ldots \text{ of form } \mathbf{QU} \text{ with } \mathbf{U} = \sqrt{\mathbf{F}^T\mathbf{F}}$$

- Kinematic compatibility at interfaces

twin boundaries: $\mathbf{A}-\mathbf{B} = \mathbf{a}\otimes\mathbf{n}$

habit planes: $x\mathbf{A}+(1-x)\mathbf{B} = \mathbf{I}+\mathbf{b}\otimes\mathbf{h}$

junction planes: $\left(x_1\mathbf{A}+(1-x_1)\mathbf{B}\right)-\left(x_2\mathbf{C}+(1-x_2)\mathbf{D}\right) = \mathbf{c}\otimes\mathbf{m}$

Ball and James (1987); Bhattacharya (2003)

Deformation gradient and variants of B19´ NiTi

Simple shear Normal stretches

$$\mathbf{F}=\begin{pmatrix}1 & 0 & 0\\ \cot(\gamma_m) & 1 & 0\\ 0 & 0 & 1\end{pmatrix}\begin{pmatrix}\sin(\gamma_m)\,a_m/\sqrt{2}a_c & 0 & 0\\ 0 & b_m/a_c & 0\\ 0 & 0 & c_m/\sqrt{2}a_c\end{pmatrix}=\begin{pmatrix}1.0796 & 0 & 0\\ -0.1475 & 0.9612 & 0\\ 0 & 0 & 0.9634\end{pmatrix}$$

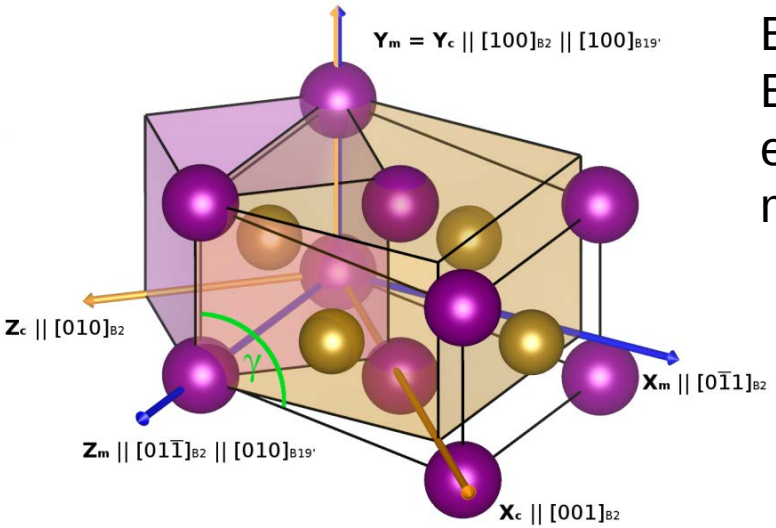

Cubic B2 austenite to monoclinic B19´ martensite

Based on crystal symmetry, there are 12 different Bain correspondance variants (BCV) with eigenstrains described by their transformation stretch matrices **U**.

$$\mathbf{U}_i=\sqrt{\mathbf{F}_i^T\mathbf{F}_i},\ i=1,\ldots,12$$

$$\mathbf{U}_1=\begin{pmatrix}\theta & \tau & \tau\\ \tau & \sigma & \rho\\ \tau & \rho & \sigma\end{pmatrix},\ \mathbf{U}_2=\begin{pmatrix}\theta & -\tau & -\tau\\ -\tau & \sigma & \rho\\ -\tau & \rho & \sigma\end{pmatrix},\ldots.$$

Hierarchical structure of martensite

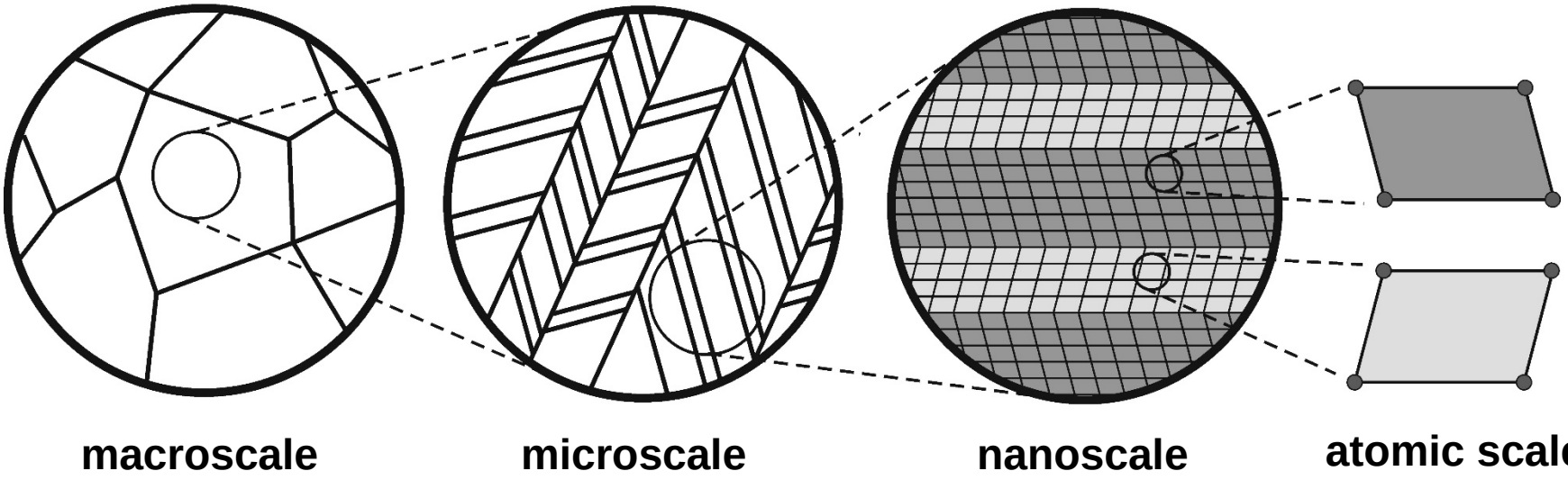

- The evolution of the structure of martensite depends on complex autocatalytic (i.e. self-triggered) processes of minimizing strain (and interfacial) energy.
- These mechanisms are dependent on geometrical (size) constraints (obstacles) such as grain boundaries.

Size constraints

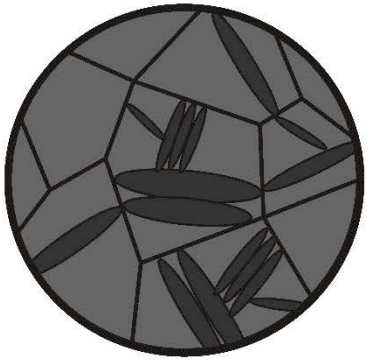

Grain boundaries

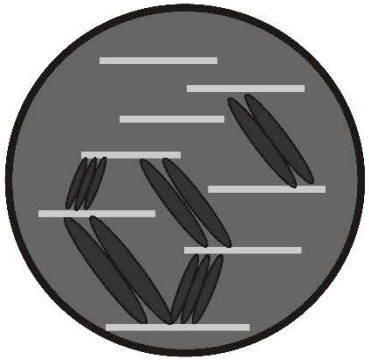

Precipitates

Partitioning

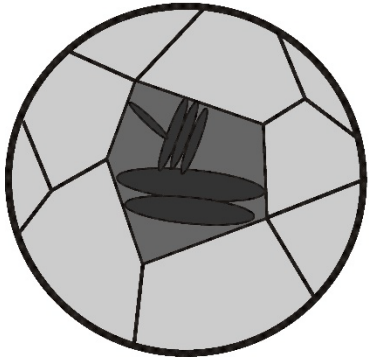

Retained austenite

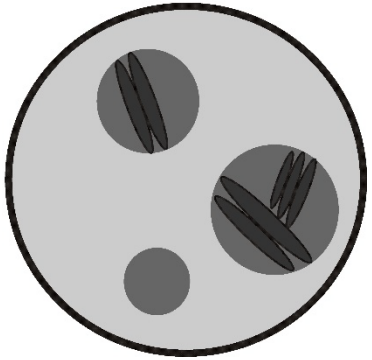

Austenitic crystallites

Experiment: how to process nanocrystalline NiTi

High pressure Torsion (HPT)

Pressure: 4 - 10 GPa
Up to ~ 100 turns

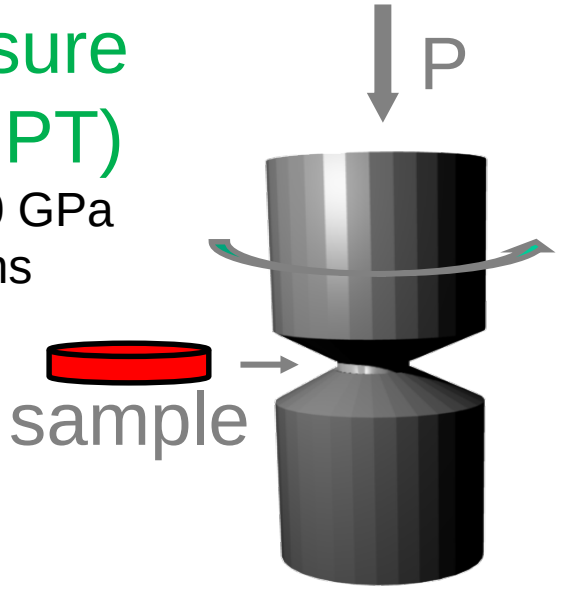

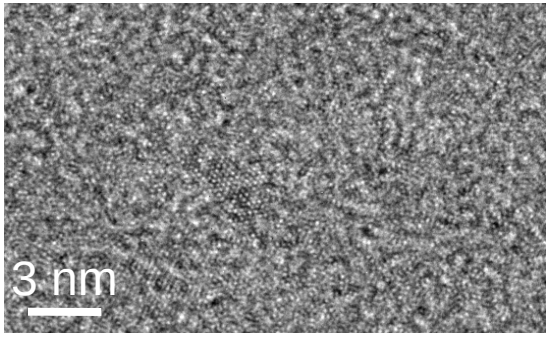

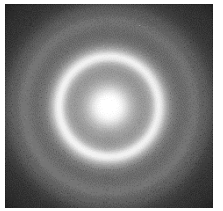

Amorphous phase

Amorphization is followed by nanocrystallization

HPT of NiTi yields amorphization

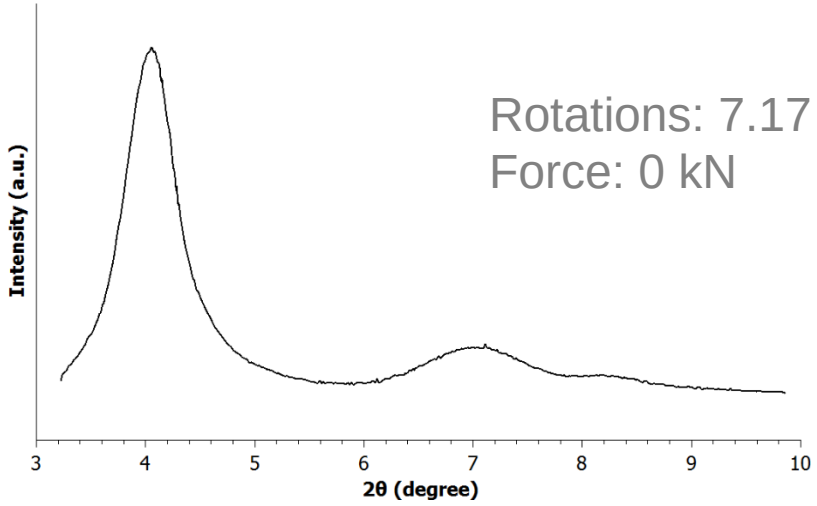

Rotations: 7.17
Force: 0 kN

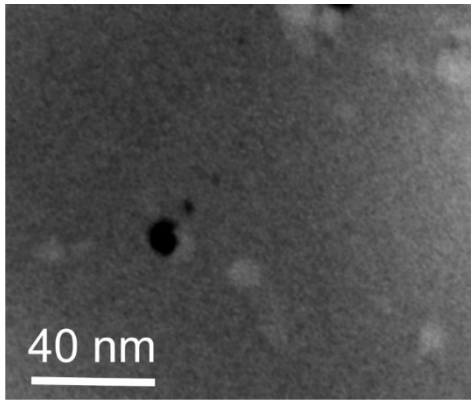

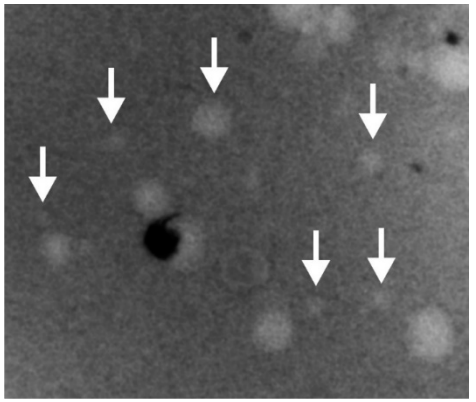

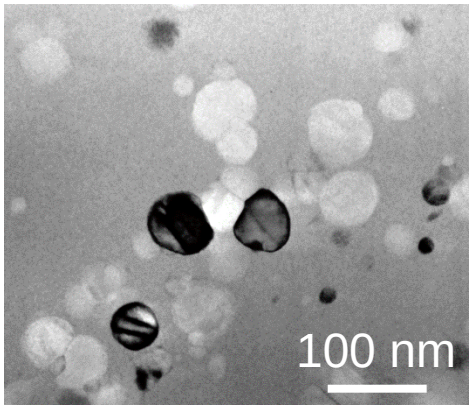

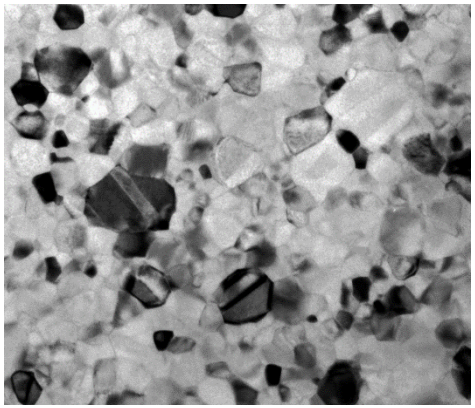

Experiment: in-situ transformation of a NiTi nanocrystal

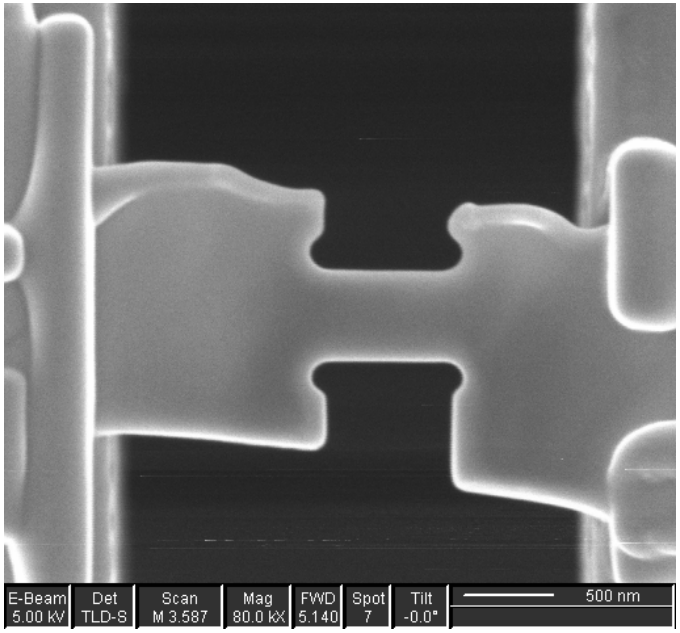

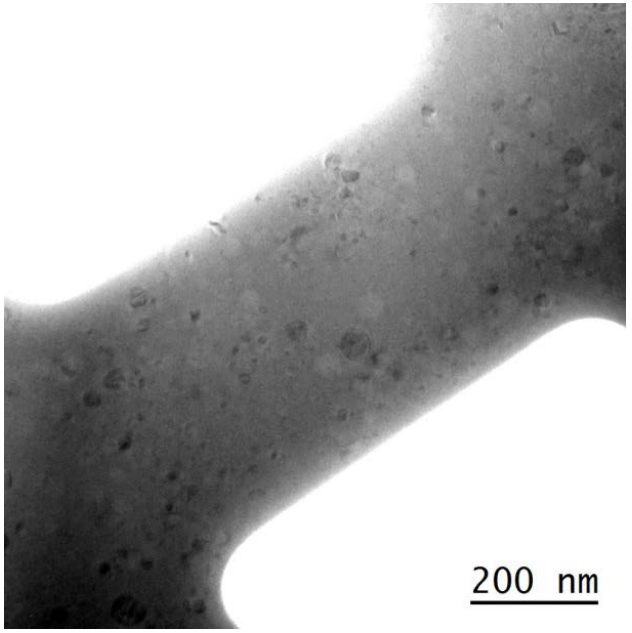

- TEM specimen obtained by a combination of electropolishing and focused ion beam (FIB) processing
- Mounting at a push-to-pull MEMS device
- In-situ recording of stress induced structural changes and the load-displacement curve

Experiment: in-situ transformation of a NiTi nanocrystal

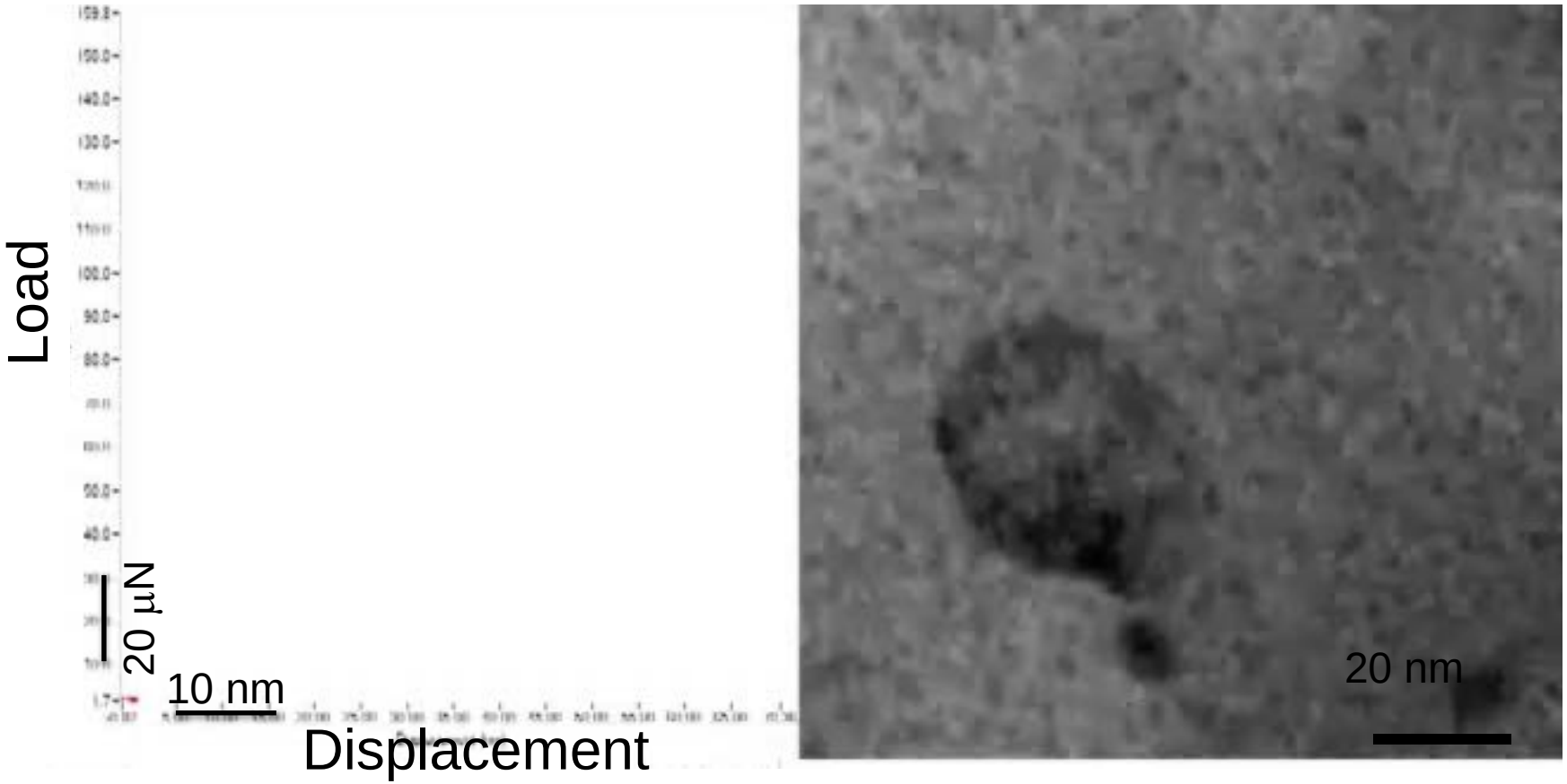

Experiment: ex-situ transformation of NiTi nanograins

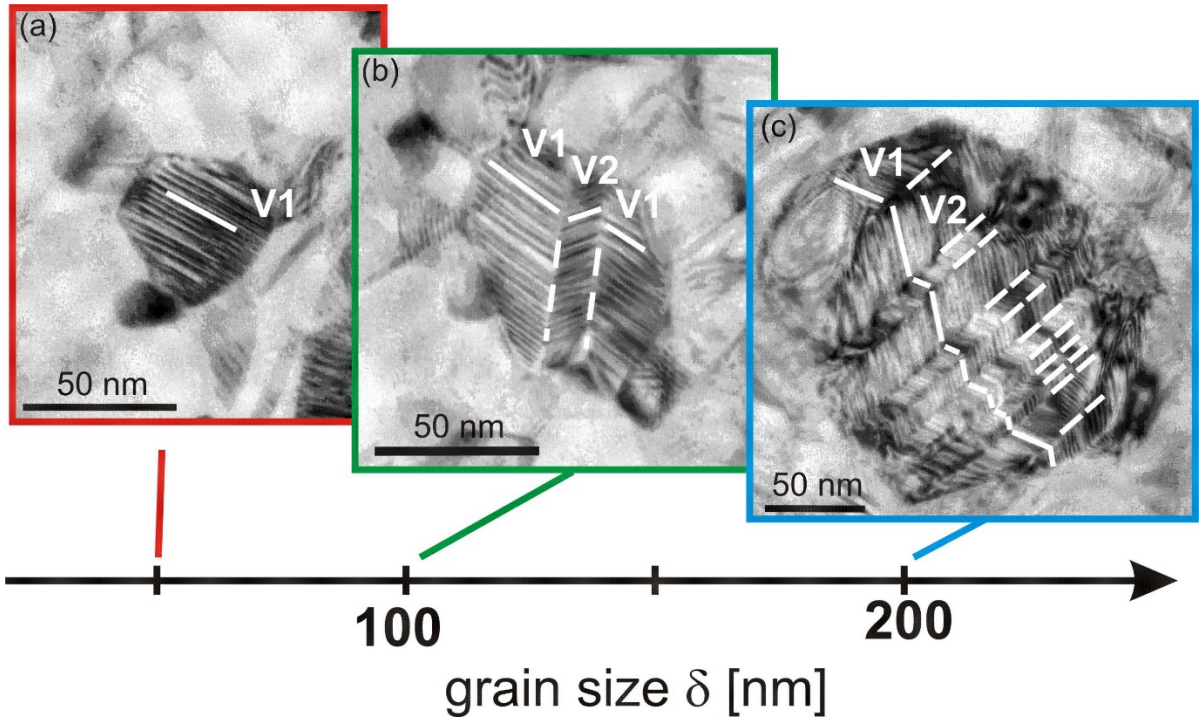

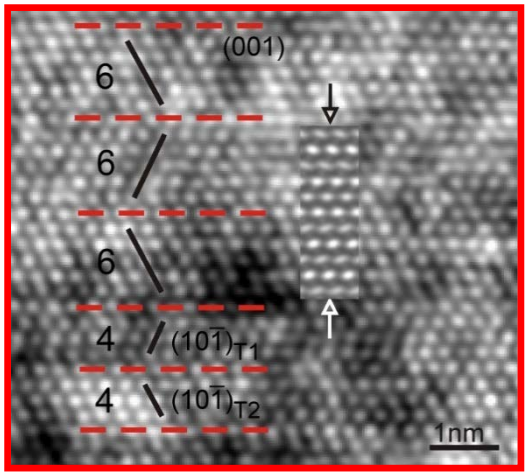

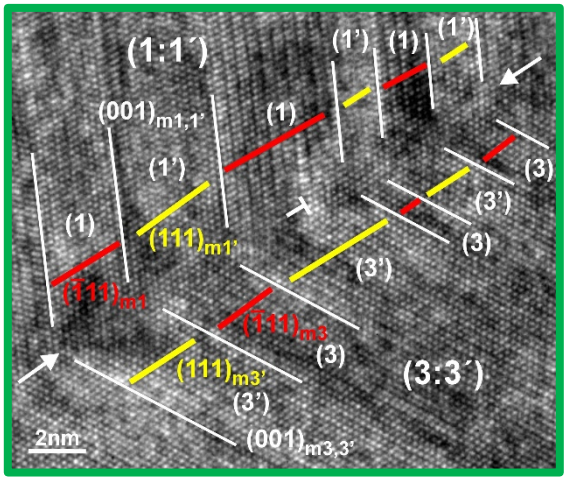

(001) compound twinned B19´ martensite is observed in the nanograins. With increasing grain size, the single twinned morphology (laminate) becomes less favorable and a herring-bone morphology prevails.

Deformation gradient and variants of NiTi

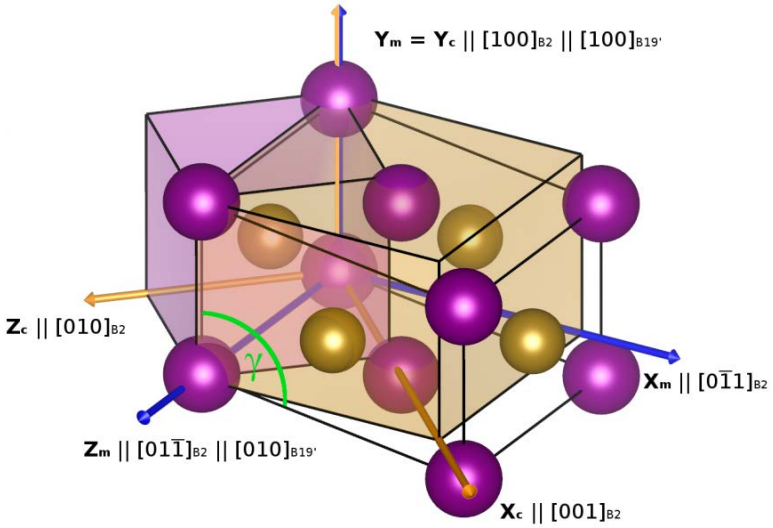

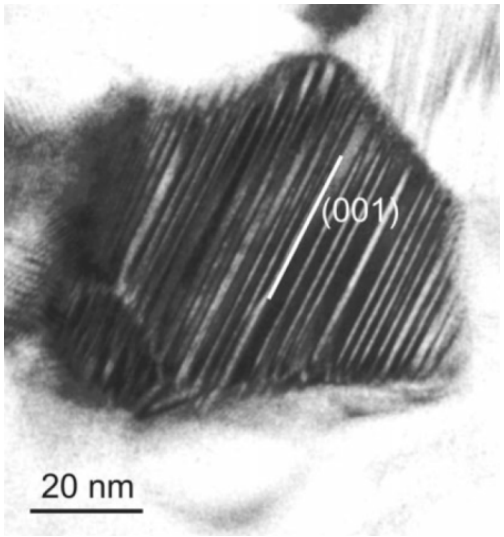

- Compound twinned variants have opposite shear components of their deformation gradients
- There are six possible compound twin variants {i, i´}
- For the deformation gradient of the laminate $\mathbf{F}^L$, the average deformation gradient is used
- As a measure of the eigenstrains of the laminate, the corresponding Green–Lagrange transformation strain tensor $\mathbf{E}^L$ is calculated

$$\mathbf{F}_i^L = \frac{1}{2}\left(\mathbf{F}_i + \mathbf{F}_{i'}\right), \quad \mathbf{E}^L = \frac{1}{2}\left(\mathbf{F}^T\mathbf{F} - \mathbf{I}\right)$$

$$\det\left(\mathbf{F}_i^L\right) = 0.9998$$

Scaling of lamellar twin pattern without branching

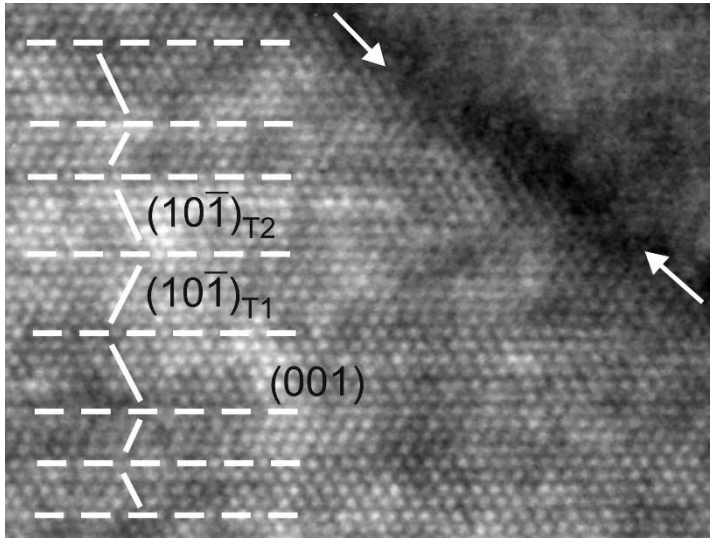

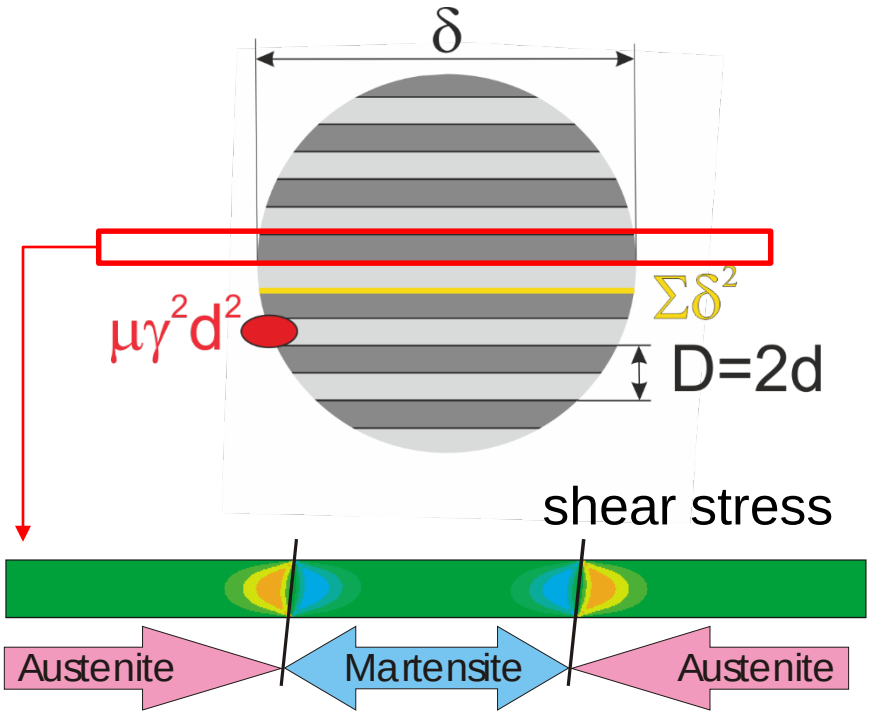

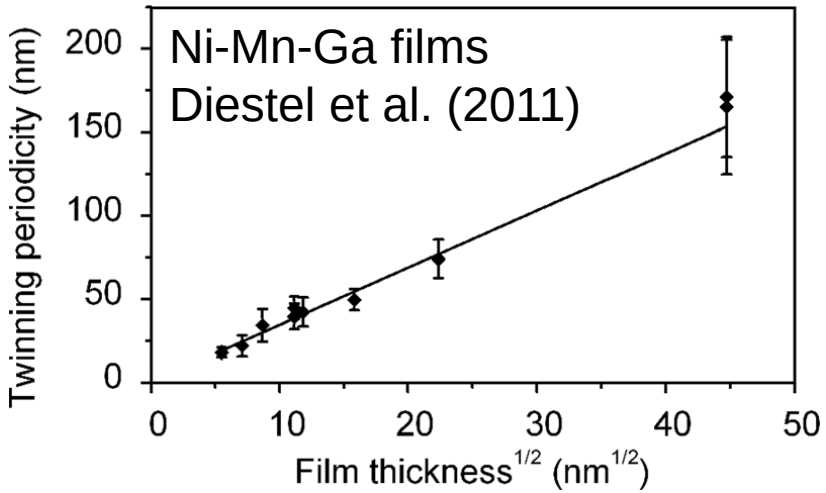

$$\Gamma_{tw} \propto \mu\gamma^2 d^2\delta\,(\delta/d)$$

$$\Gamma_{in} \propto \Sigma\delta^2(\delta/d)$$

$$d \propto (\Sigma/\mu\gamma^2)^{1/2}\ \delta^{1/2}$$

Energy of the transformation of a single grain

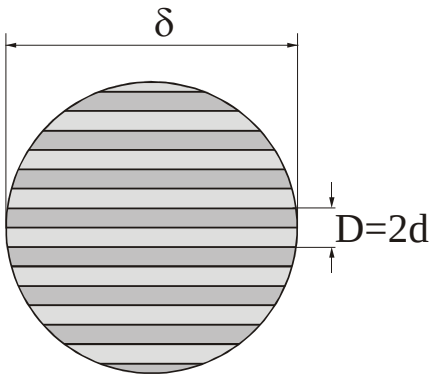

Gibb´s free enthalpy difference : $\Delta g = \Delta g_c + \Delta g_{nc}$

Transformation condition : $\Delta g \leq 0$

Chemical driving force : $\Delta g_c = g_c^M - g_c^A$,

for small undercooling: $\Delta g_c = \Delta s \cdot (T_0 - T)$

Energy barrier : $\Delta g_{nc} = (\underbrace{\Gamma_{tw}}_{\sim d} + \underbrace{\Gamma_{in}}_{\sim \delta/d} + \underbrace{\Sigma_s}_{\sim 1/\delta})\frac{A}{V} + u + f_c$

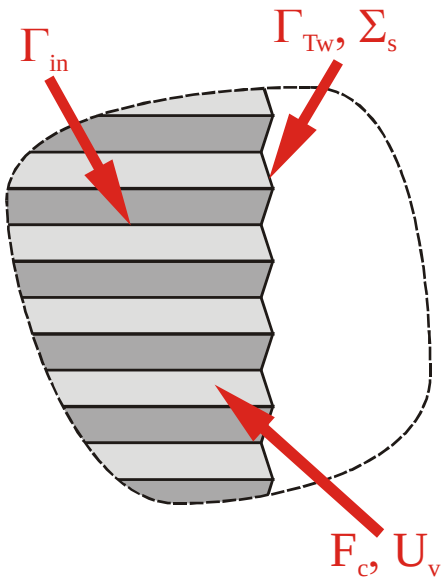

Fe modeling of the transformation of single grains

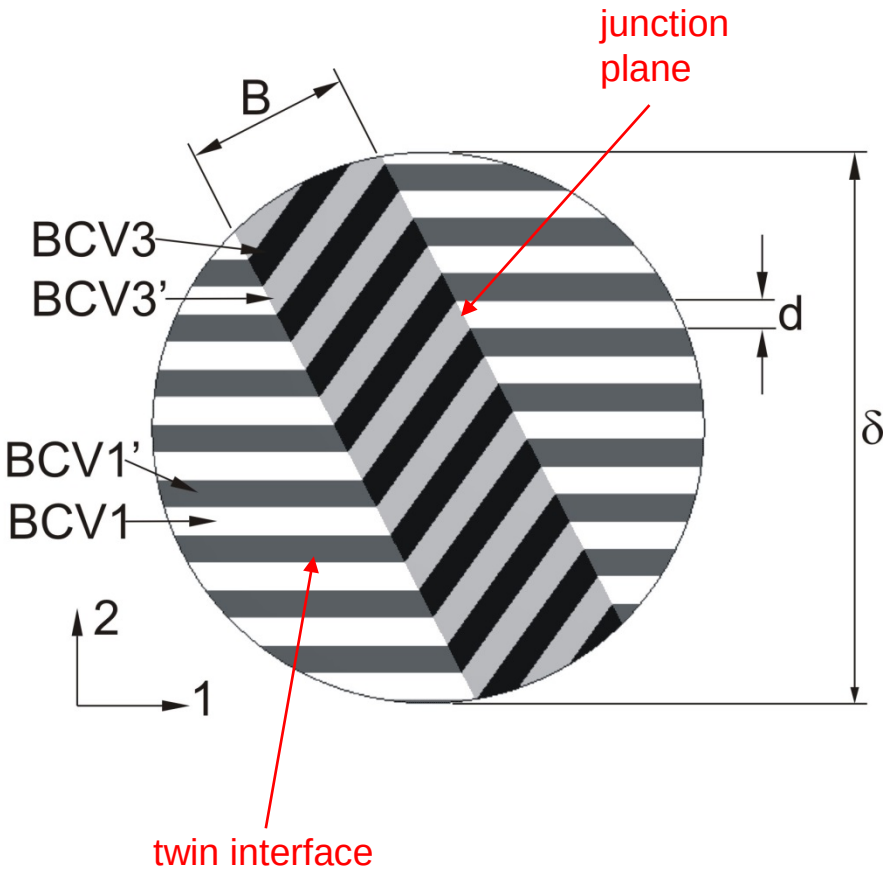

250.000 tetrahedral elements
with quadratic shape functions

Modeling parameters

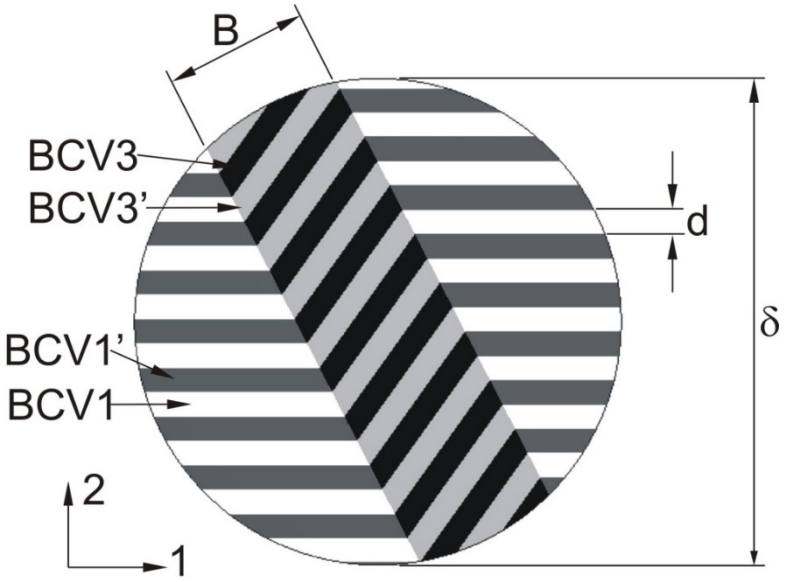

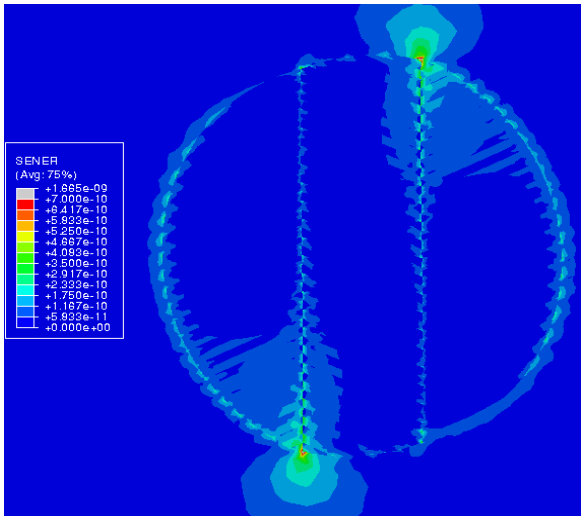

- Volumetric (*U*) and interfacial contributions (Γ_{tw}) to the strain energy were calculated using FE for different morphologies (single laminate, herring-bone), grain sizes δ, and twin widths d.
- A specific twin boundary energy of 0.014 J/m^2 was calculated by ab-inito methods.
- The variant geometry fully reflects the invariant junction plane condition.
- A full set of anisotropic elastic constants was used for the martensite (averaged over the compound twins).
- Frictional work f_c~6 10^6 J/m^3 was taken from the literature, the chemical boundary energy of the martensite/austenite interface and the junction planes was assumed to be Σ_s=0.1 and 0.15 J/m^2, respectively.

Results of modeling of a single-grain transformation

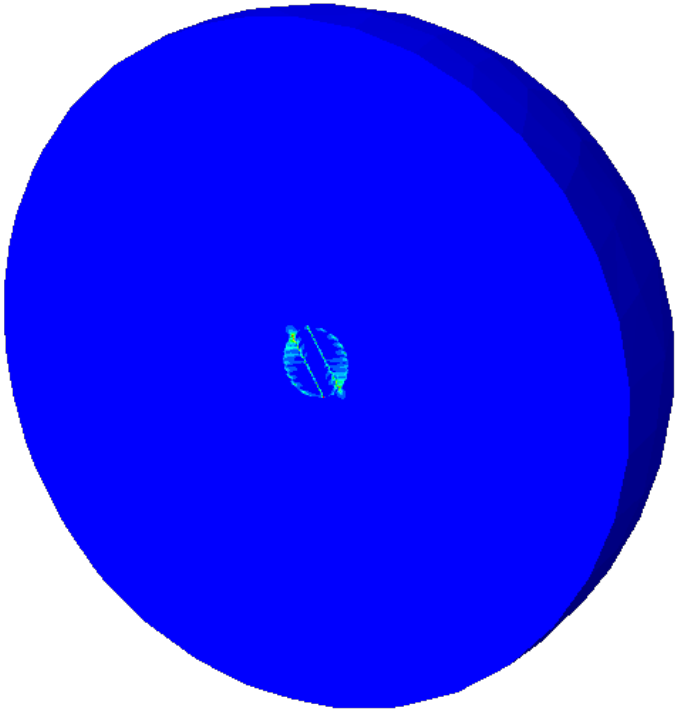

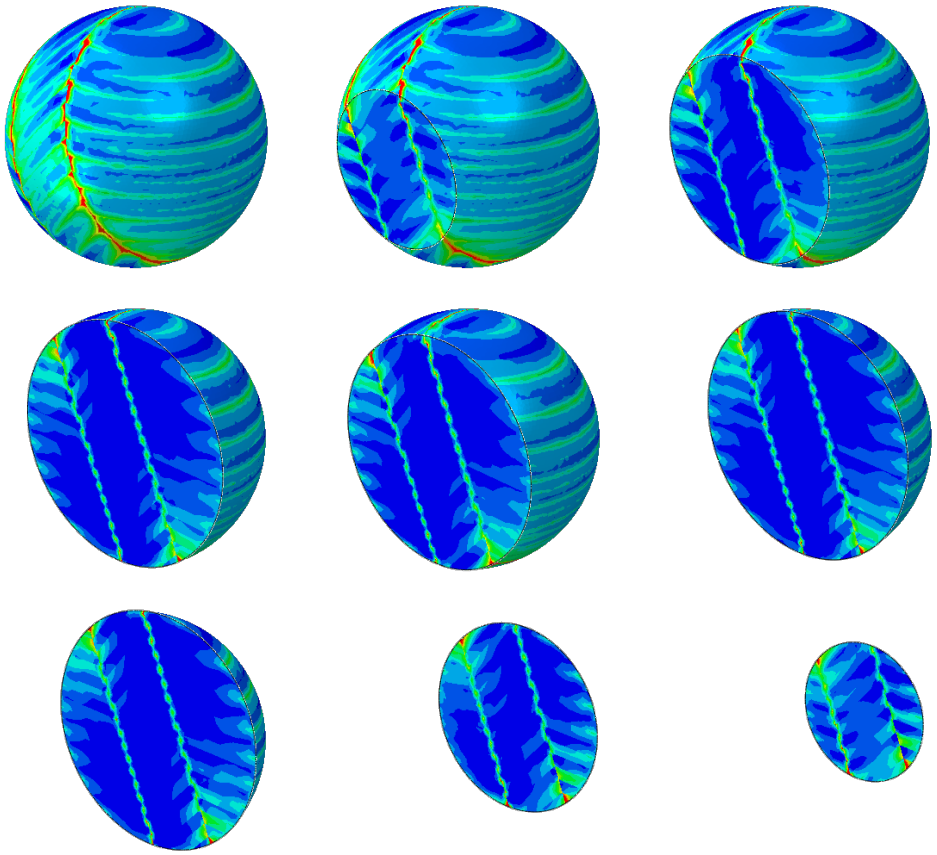

transformed martensitic grain embedded in a matrix of austenite

Scaling of the energy barrier

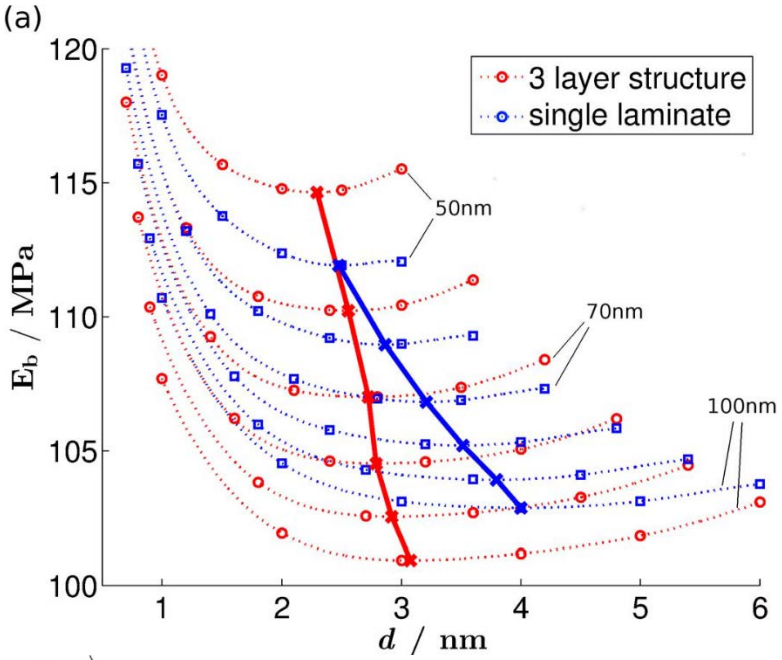

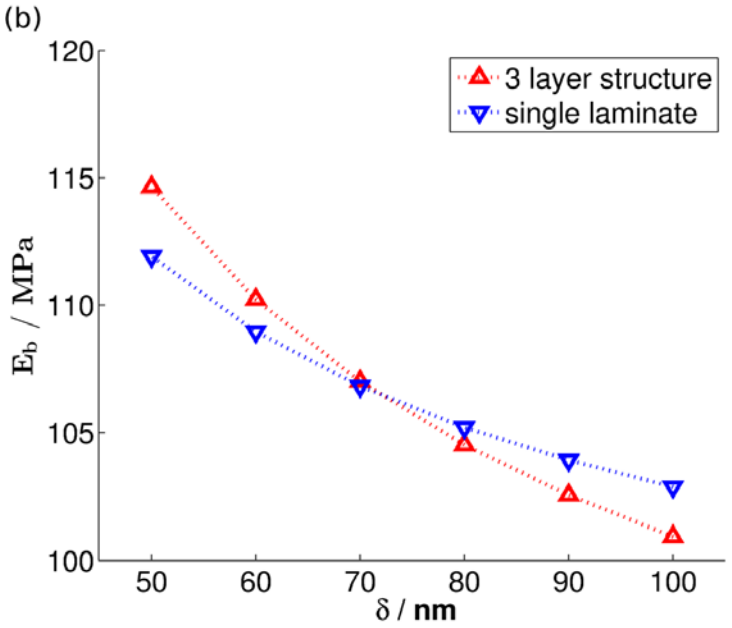

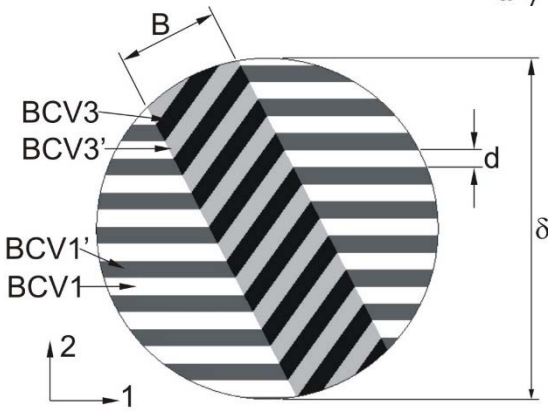

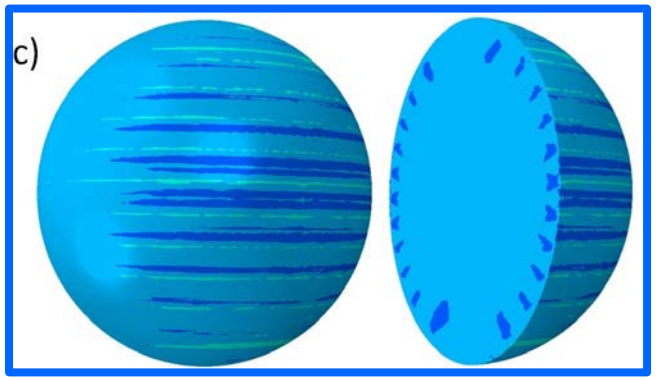

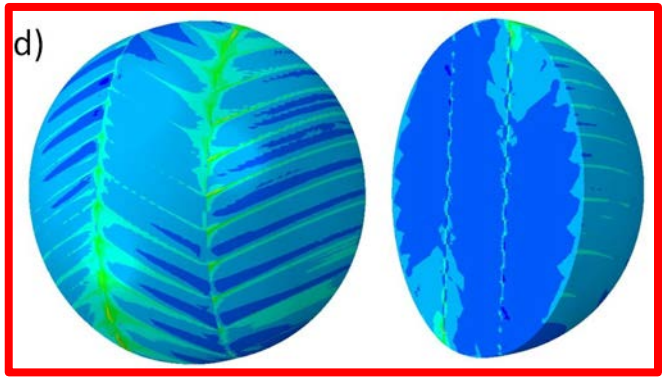

Single laminate

3-layer herring bone

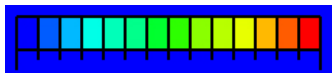

Strain energy density

Martensite formation in a polycrystalline aggregate

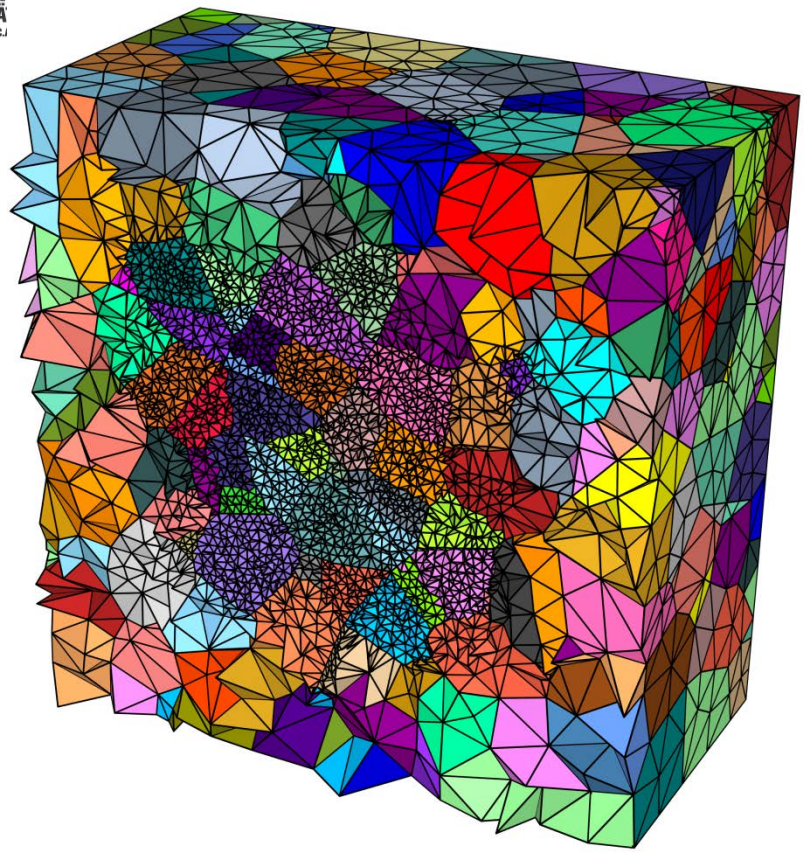

M. Petersmann *et al. (*2017)
Modelling Simul. Mater. Sci. Eng. **25**

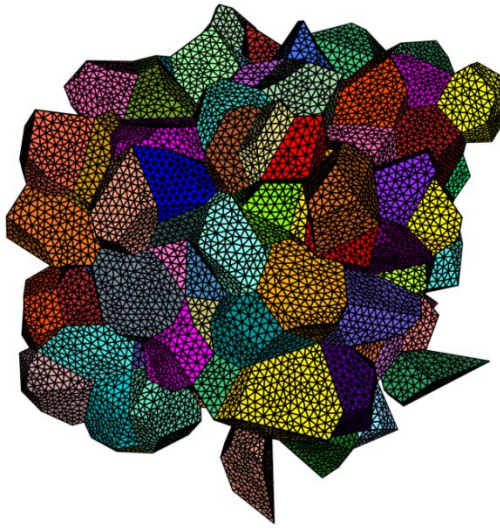

Transformation occurs in the RVE

- The volume is split into a surrounding matrix and an inner representative volume element (RVE).
- All grains of the RVE are smaller than 80 nm. Therefore, a single laminate morhpology is considered only.

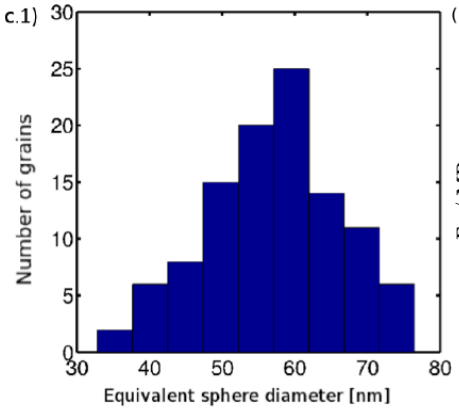

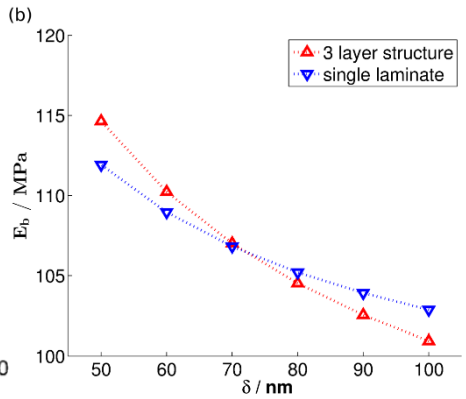

Incremental energy minimization algorithm (IEMA)

Given
N grains in the RVE (here 107),
v compound twinned variants (v=6),
k grains already transformed,
there are (N-k)v possibilities for the next transformation step (i.e. which grain i will transform into which variant v_i).

The selection criterion of (i, v_i) is based on the minization of the increment in the energy barrier (ε_k) opposing the transformation in each step k.

In each step, the energy barrier is calculated by FE using the semianalytical model of a single grain taking the elastic interactions of neigbouring grains into accout. I.e. selecting the (i, v_i) minimizing the total free energy of the polycrystalline aggregate (for N=107, about 35000 FE calculations are necessary).

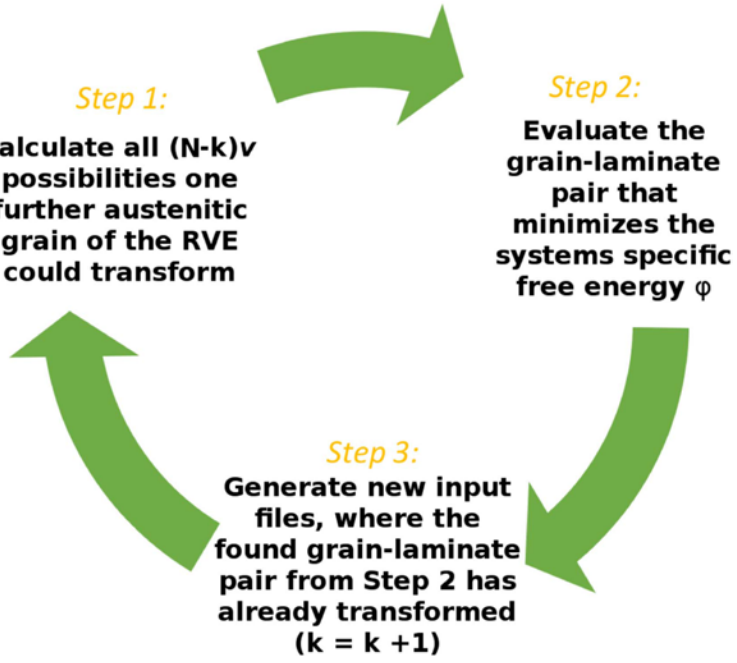

Transformation sequence in the polycrystalline aggregate

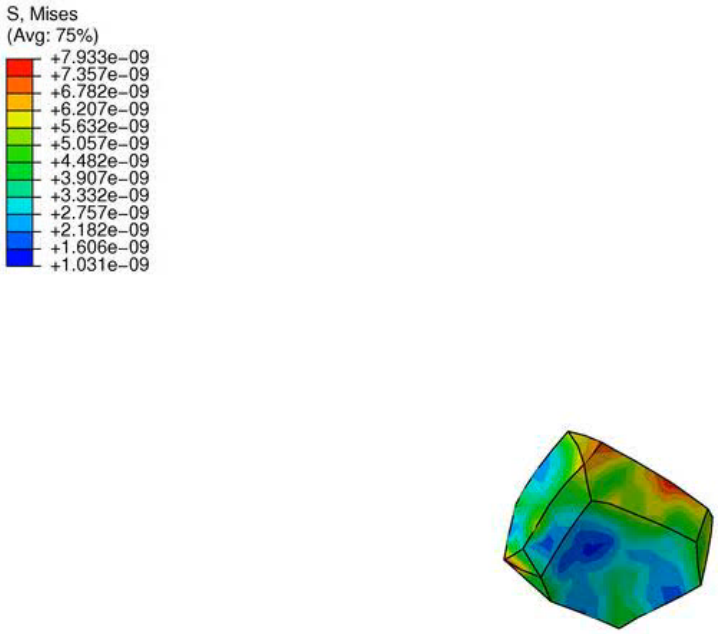

Autocatalytic effects

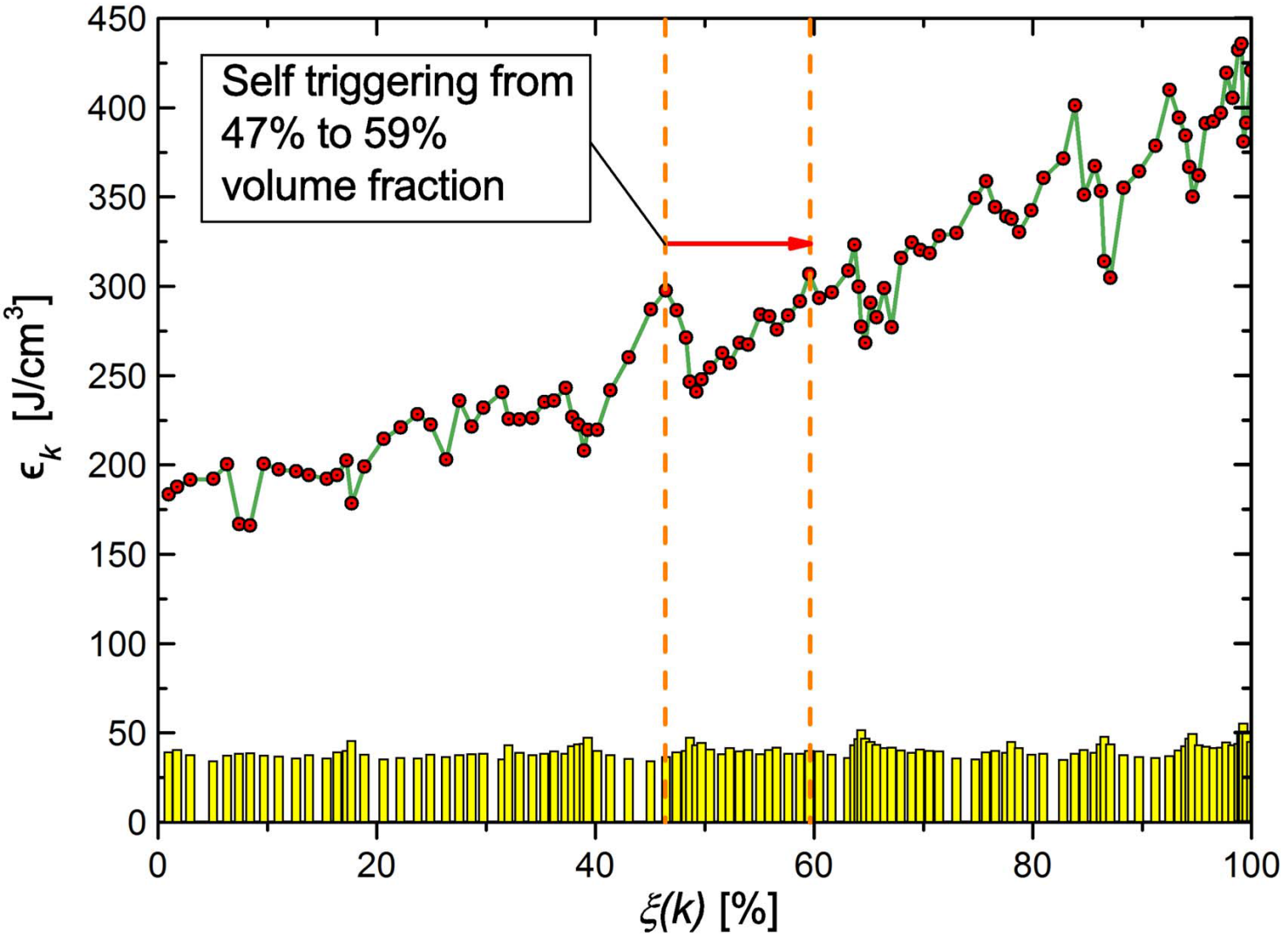

Strain energy distribution for about 50% of transformation

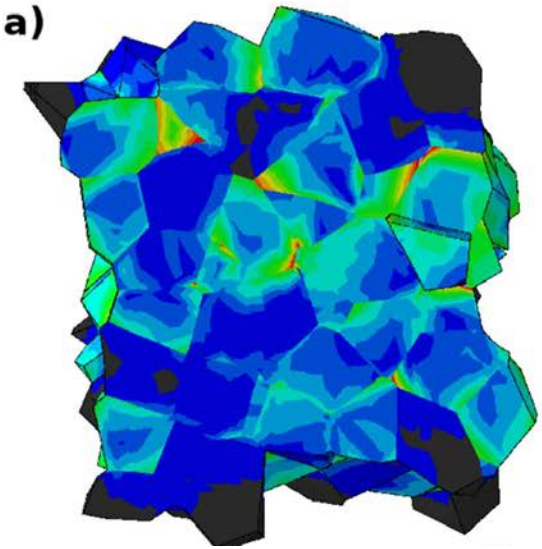

Total RVE
($\xi(k) \sim 0.5$)

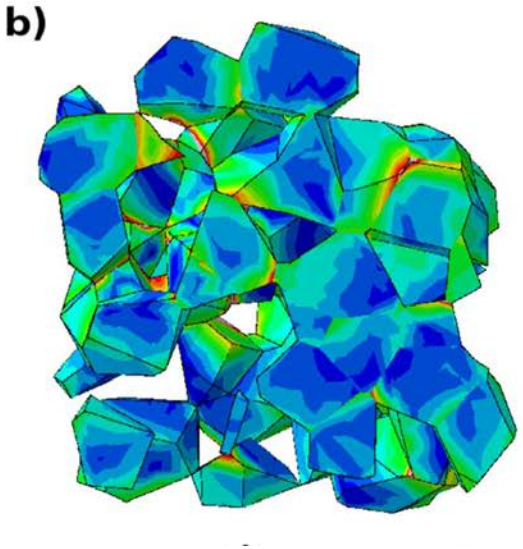

Martensitic grains

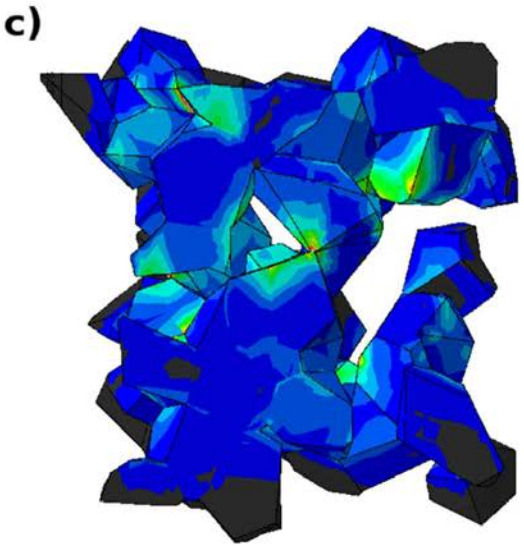

Austenitic grains

Energy of RVE as function of its martensitic fraction

Strain energy

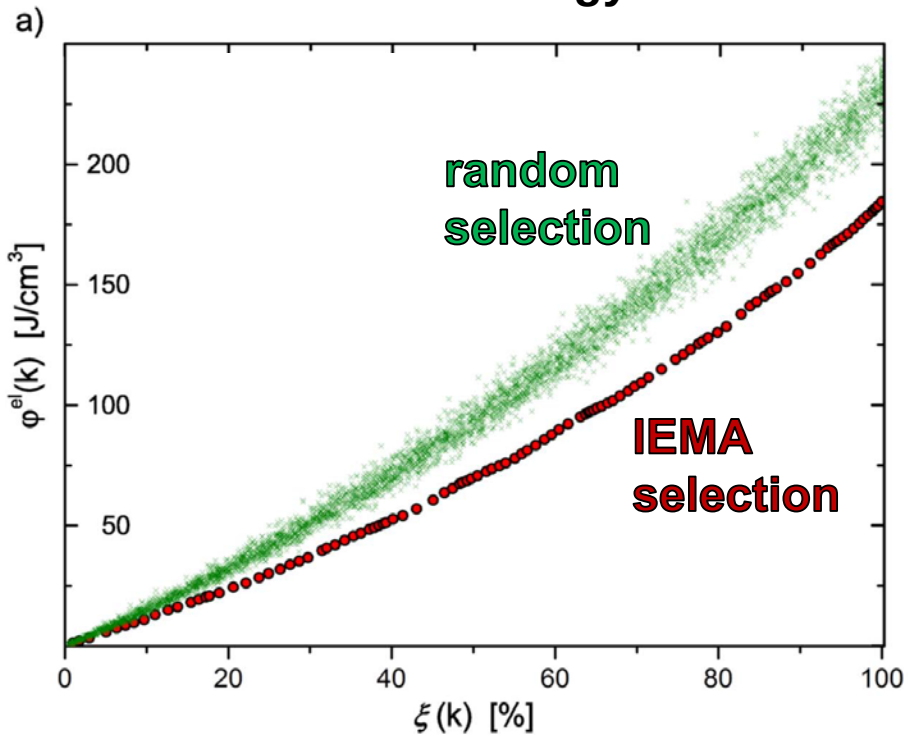

Strain & interface energy

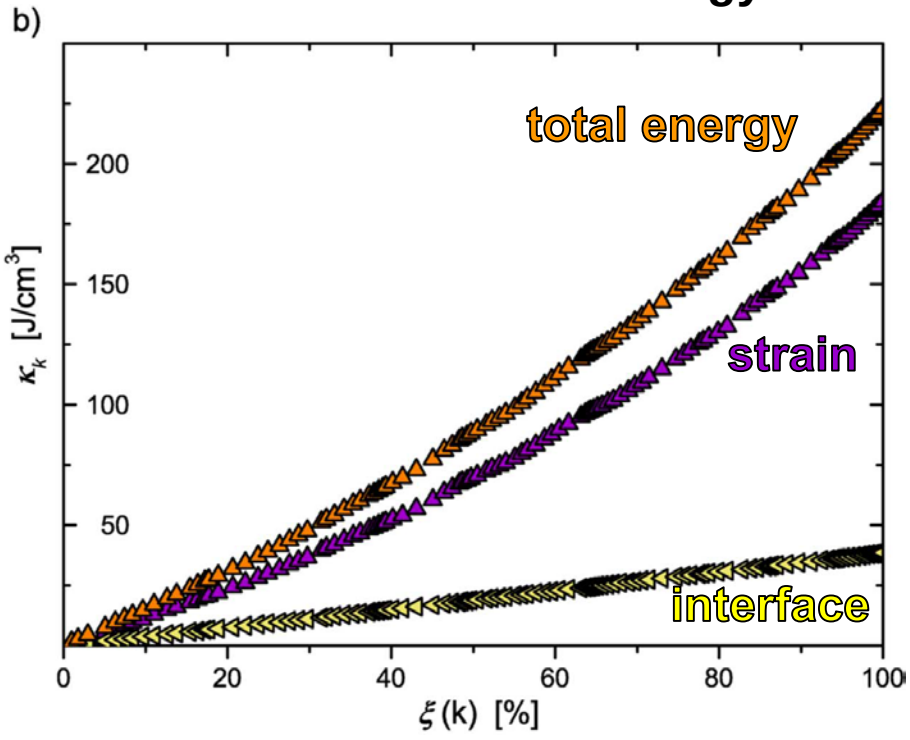

Martensitic fraction as a function of chemical driving force

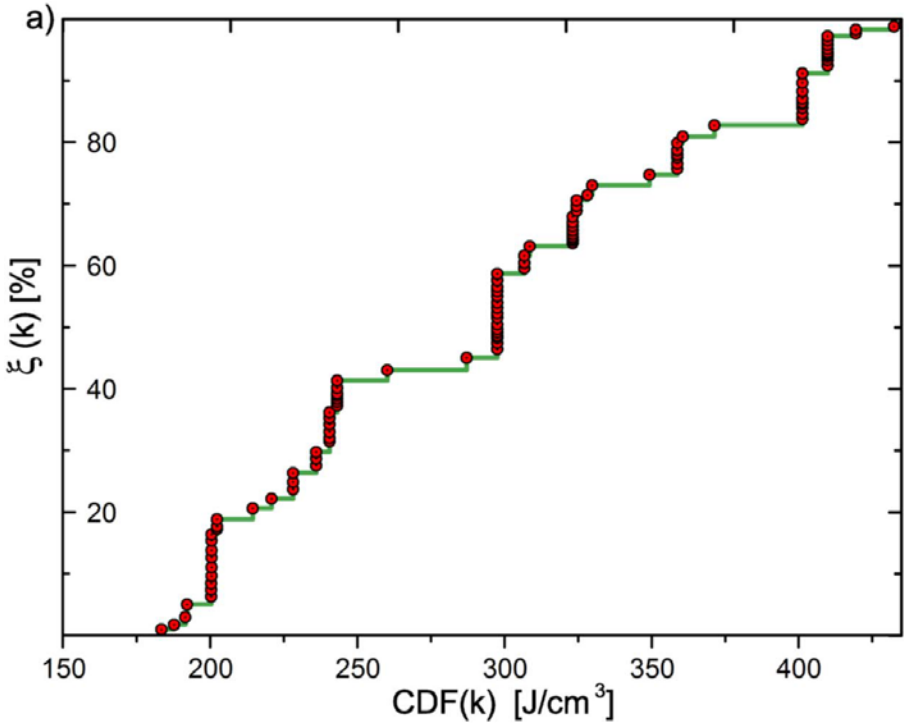

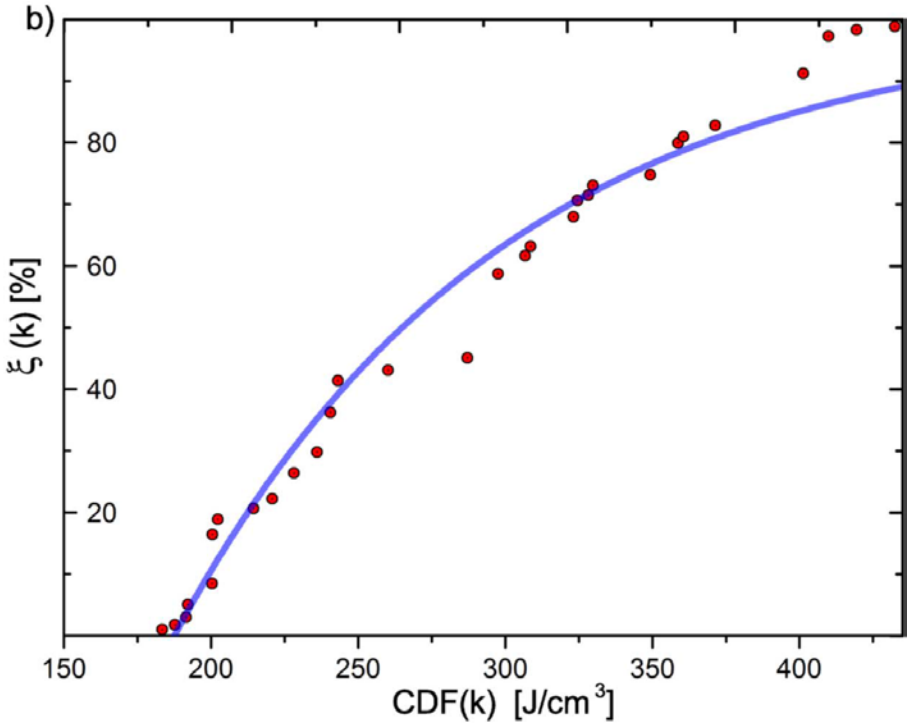

Koistinen Marburger kinetics

$$\xi = 1 - \exp\left(a \cdot CDF\right)$$

$$= 1 - \exp\left(a' \cdot \left(M_s - T\right)\right)$$

Conclusions

- Nanocrystalline NiTi has been processed by severe plastic deformation and a post deformation heat treatment leading to amorphization followed by crystallization.
- The self-accommodated morphology of compound twinned martensite was analyzed at an atomic scale by TEM.
- Modelling allows quantification of the various energies that decide upon the morphology of the twin banded microstructure.
- Interaction effects in polycrystals and the phenomenon of self triggering have been quantified. Self triggering has a significant impact on the transformation kinetics.